Pergamon

1359-6454(95)00438-6

Acta mater. Vol. 44, No. 8, pp. 3331–3338, 1996

Published by Elsevier Science Ltd

1359-6454/96 $15.00 + 0.00

THE HAFNIUM–NITROGEN SYSTEM: PHASE EQUILIBRIA AND NITROGEN DIFFUSIVITIES OBTAINED FROM DIFFUSION COUPLES

W. LENGAUER, D. RAFAJA, G. ZEHETNER and P. ETTMAYER

Institute for Chemical Technology of Inorganic Materials, Vienna University of Technology, Getreidemarkt 9, A-1060 Vienna, Austria

(Received 18 September 1995)

Abstract—Hafnium sheet and wedges were annealed in nitrogen atmosphere at temperatures of 1160–1800°C and nitrogen pressures of 1–30 bar. The *in situ* diffusion couples were used to study the phase equilibria in the Hf–N system and for the determination of nitrogen diffusivities in η-Hf_3N_{2-x}, ζ-Hf_4N_{3-x} and δ-HfN_{1-x}. The activation energy of the nitrogen diffusion process is 2.7 eV in all three phases indicating an identical diffusion mechanism (migration via octahedral nitrogen vacancies). It is shown that wedge-type diffusion couples can be used to measure homogeneity regions of line compounds (e.g. by EPMA) more accurately. A corrected version of the hafnium–nitrogen phase diagram is presented which contains better information on the homogeneity ranges of η-Hf_3N_{2-x} and ζ-Hf_4N_{3-x}. The present study showed that previous investigations which place the lower stability limit of ζ-Hf_4N_{3-x} at around 1200°C were in error due to the low rate of layer growth of this phase by diffusion at low temperatures. ζ-Hf_4N_{3-x} is indeed stable at $T < 1200$°C. At high pressures and/or lower temperatures δ-HfN_{1-x} forms a diffusion band which has a metallographic double-layer appearance because of the formation of hyperstoichiometric δ-HfN_{1+x} on δ-HfN_{1-x}. Copyright © 1996 Acta Metallurgica Inc.

1. INTRODUCTION

The hafnium nitride phase δ-HfN_{1-x} is a hard, high-melting, yellow compound and hence has attracted interest for use as a protective layer in technical and ornamental applications [1]. Nevertheless, only a very few studies have been performed to establish the phase equilibria in the Hf–N system.

Rudy [2] observed two subnitride phases, η-Hf_3N_{2-x} (originally named ϵ-Hf_3N_{2-x}) and ζ-Hf_4N_{3-x}, after a reinvestigation of his first results [3] in which a "Hf_2N" phase had been proposed. He determined the crystal structures of these subnitride phases, gave their average compositions, which deviate from the ideal 3/2 and 4/3 stoichiometry, respectively, and reported their approximate upper stability temperatures. Billy and Teyssedre [4] carried out nitriding experiments with Hf sponge and plates at temperatures up to 1220°C. ζ-Hf_4N_{3-x} was detected neither in the metallographically prepared plates nor in the sponge or heat-treated Hf/HfN powder mixtures by XRD. Possibly the reaction times (about 4 h for the investigation of nitridation kinetics for T up to 1000°C and about 100 h for the powder mixture heat treatment) were too short to produce a sufficient amount of ζ phase for observation by metallography (performed on plates) or XRD (performed on powder samples). Alternatively, it could be that the ζ phase does not form at all in this temperature range. Recently it was possible to measure the average composition of η-Hf_3N_{2-x} and ζ-Hf_4N_{3-x} by GC-Dumas analysis since both phases could be prepared in single-phase form by means of diffusion couples [5].

Results for the δ-HfN_{1-x} phase were reported by Rudy and Benesovsky [3]. The lattice parameter of this f.c.c. phase was reported to decrease slightly with increasing nitrogen content up to [N]/[Hf] = 1.00 and then sharply at hyperstoichiometric compositions, probably due to the formation of vacancies in the metal sublattice [6]. The hyperstoichiometric composition up to 52 at% N can be reached by annealing Hf metal in nitrogen—a phenomenon which, for instance, is not observed in the Ti–N system where a nitrogen concentration above 50 at% N in equilibrium with nitrogen apparently can only be achieved by reacting $TiCl_4$ with ammonia.

Recently, the hafnium–nitrogen system was reviewed [7, 8]. The latest article by Okamoto [7] is, however, in error regarding the true compositions of the subnitride phases as reported by Rudy [2]. For the stability range of ζ-Hf_4N_{3-x} a questionable lower stability limit at around 1200°C was given in the phase diagram because of the results in Billy and Teyssedre [4].

In view of the insufficient data on the phase equilibria as well as the absence of any diffusivity data in the Hf–N system, it was decided to perform a study based on diffusion couples which yield both chemical diffusivities and phase equilibria.

2. EXPERIMENTAL

2.1. Preparation of diffusion couples

The starting material consisted of 0.67 and 1.6 mm thick Hf sheet and a Hf bar. These had Zr contents of 2.0, 2.0 and 3.2 wt%, respectively. The thin sheet and the bar were not further characterized; the thick sheet contained 30 ppm carbon. Plates of various sizes (2×8–17×17 mm) were cut from these materials, ground with SiC paper, etched with diluted hydrofluoric acid, washed and placed in a sample holder. The latter was made by wrapping 25 μm Hf foil (which served as a getter for impurities and contained 3.5 wt% Zr) over a steel cylinder and putting two such halves together to obtain a closed container. During nitridation the Hf cylinder converted to δ-HfN. The inner windings of this nitrided cylinder did not show any traces of contamination (to which the color of HfN is very sensitive). They were very thin and hence did not have a concentration gradient. By chemical analysis of this material the surface equilibrium concentration of nitrogen in the thick couples could be determined.

In most cases a 25 μm Ta foil or pieces of a 1 mm Ta wire served as a contact barrier between Hf foil and samples in order to prevent sticking. The samples were then transferred to a cold-wall autoclave equipped with a tungsten heating tube and molybdenum radiation shields. Before heating the autoclave was evacuated/backfilled at least three times with a rotation pump using >99.999 vol% N_2. Temperatures between 1160 and 1800°C, pressures between 1 and 30 bar and reaction times of 1–1000 h, depending on the temperature, were applied. For extended heat treatments in Ar atmosphere an additional cold-wall autoclave of the same design but with a larger heating tube was used. The samples were placed in Hf foil as described above and then in a thick Mo crucible. Heating and cooling cycles in this autoclave were considerably longer than in the former one.

The temperature was measured either with a Pt30 % Rh/Pt6% Rh thermocouple, a disappearing filament pyrometer or a two-color infrared pyrometer. Temperature fluctuations were recorded during all thermocouple and two-color pyrometer runs of $T < 1700$°C and were of the order of ± 15°C. The nitrogen pressure was measured with a bourdon-type manometer and/or occasionally with a piezoelectric cell. The samples were heated in a few minutes to the reaction temperatures and afterwards cooled within about 1 min to room temperature.

2.2. Sample characterization

For XRD phase analysis as a function of depth from the surface, the samples were glued with thermoplastic resin to a stainless steel cylinder which fitted into the polishing machine and into the rotating sample holder of the XRD goniometer. Diffraction patterns were taken with Cu-K_α radiation (secondary graphite monochromator) from the stepwise diamond ground surfaces. Samples with very thin phase bands, or where only the outermost region was investigated, were etched stepwise with a water-diluted mixture of hydrofluoric acid and nitric acid in order to remove parallel layers on a micron scale. Thickness measurements were taken with a micrometric screw.

Metallographic preparation was done by cutting the samples with a diamond disc, embedding them into cold-setting resin, first grinding them with a diamond disc and then polishing them with 3 μm diamond paste followed by an aqueous SiO_2 suspension.

For electron probe microanalysis (EPMA) polished samples were used that had occasionally been coated with a thin conductive carbon layer. Wavelength-dispersive EPMA was carried out for the N-K_α, Hf-M_α and Zr-L_α lines with a Cameca Camebax SX50 microprobe equipped with five crystal spectrometers. For the measurement of nitrogen an artificial W–Si crystal (60 Å lattice spacing), for Hf a TAP crystal and for Zr a PET crystal was applied. Measurements were performed in the step scan mode (step width 2–5 μm) with 10 s counting time per step, 60–100 nA beam current and 15 kV accelerating voltage. A nitrided Hf foil or, occasionally, a single-phase η-Hf_3N_{2-x} sample which had been analyzed for nitrogen by Dumas-GC analysis [9], pure "reactor-grade" Zr as well as Hf metal (with 2 wt% Zr) were used as standards for the corresponding elements.

3. RESULTS AND DISCUSSION

3.1. Phase stabilities

Provided that the diffusion process was stopped at a stage where the core of the samples still consisted of α-Hf(N), the morphology of the diffusion couples in the temperature range 1245–1800°C was principally identical (Fig. 1). The top layer consisted of δ-HfN_{1-x}, which, depending on the nitrogen pressure sometimes had a double-layered appearance (see below). Below the top layer a narrow phase band of ζ-Hf_4N_{3-x} was followed by a broad band of η-Hf_3N_{2-x}.

At temperatures below 1245 ± 25°C (the temperature interval is given by the size of the temperature steps) the phase band of ζ-Hf_4N_{3-x} could not be detected as a diffusion band. At a first glance this finding is consistent with the results of Billy and Teyssedre [4], who performed annealing experiments and subsequent metallographic investigation of Hf plates at $T = 1220$°C with unspecified annealing times (these were reported only for temperatures up to 1000°C where the annealing time was 4 h, which would be too short to observe a ζ-Hf_4N_{3-x} diffusion band by light-optical methods even if it did form). A sample calculation for 1220°C with diffusion coefficients from the Arrhenius plot given below yields a ζ-Hf_4N_{3-x} phase band thickness of 0.45 μm for an

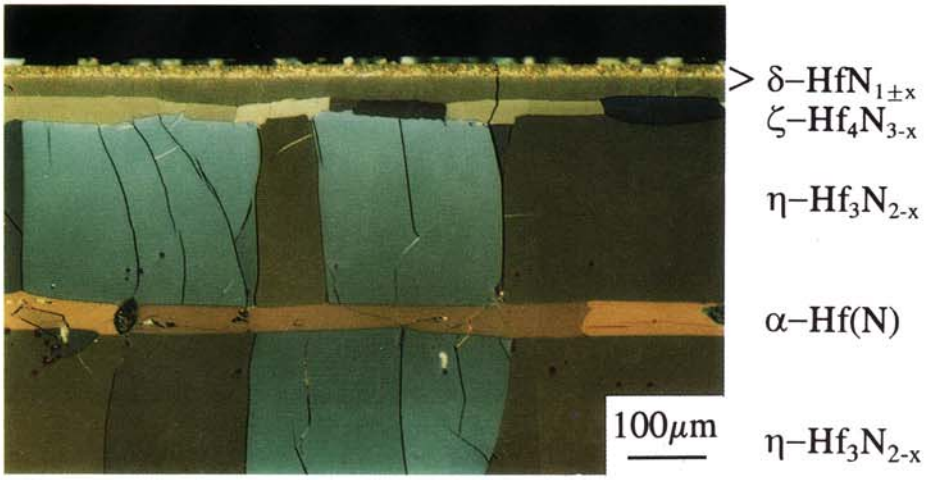

Fig. 1. Microstructure of a diffusion couple annealed at 1400°C showing the phases δ-HfN_{1-x} (double band), ζ-Hf_4N_{3-x} and η-Hf_3N_{2-x} together with an α-Hf(N) core. Note the large difference in band widths of the structurally closely related phases ζ-Hf_4N_{3-x} and η-Hf_3N_{2-x}. Polarized light.

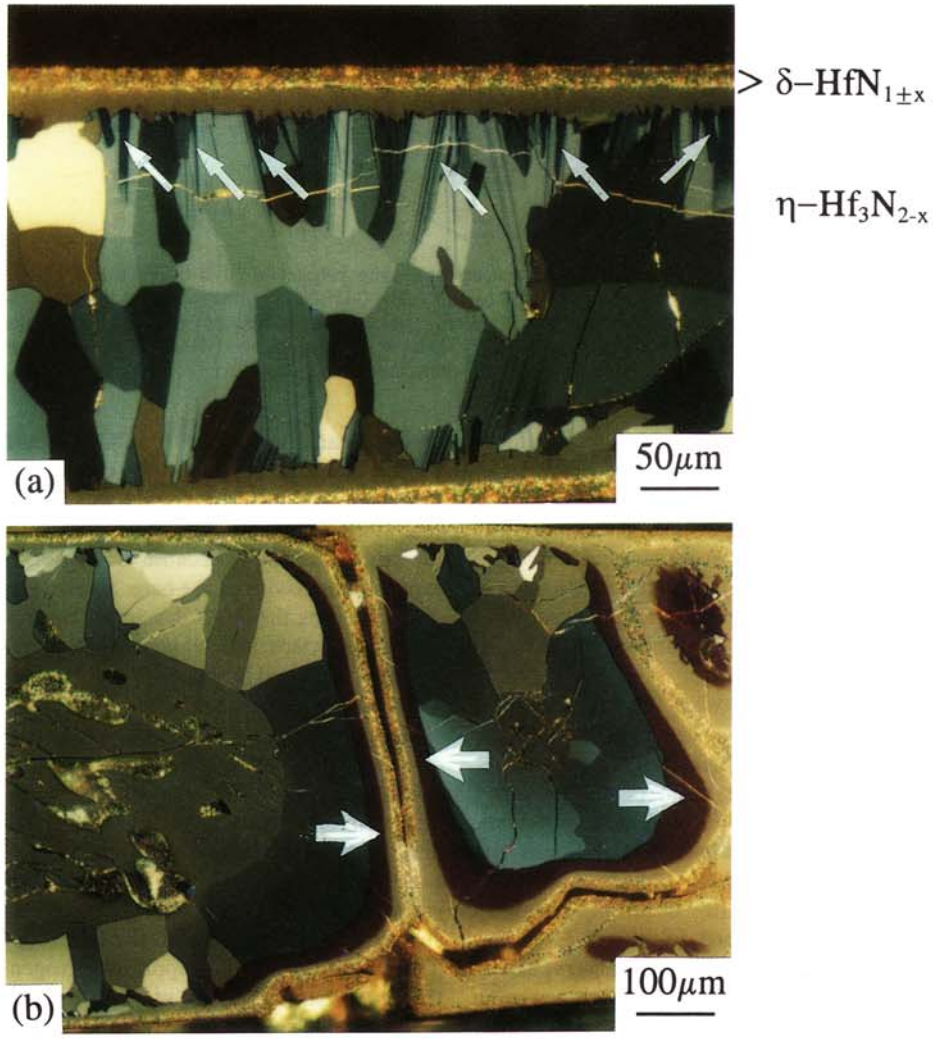

Fig. 2. Microstructures of selected sections of a wedge-shaped diffusion couple annealed at 1160°C. Polarized light. (a) At positions where the sample did not crack, the ζ-Hf_4N_{3-x} phase formed only some individual grains and hatched structures (arrows) and did not form a diffusion band. (b) At positions where the wedge was thicker the sample cracked and the nitrogen could also diffuse in a lateral direction (arrow). The ζ-Hf_4N_{3-x} phase formed in the original main diffusion direction (vertical) in a hatched structure [compare Fig. 2(a)] whereas in lateral diffusion direction (horizontal) a continuous ζ-Hf_4N_{3-x} phase band formed.

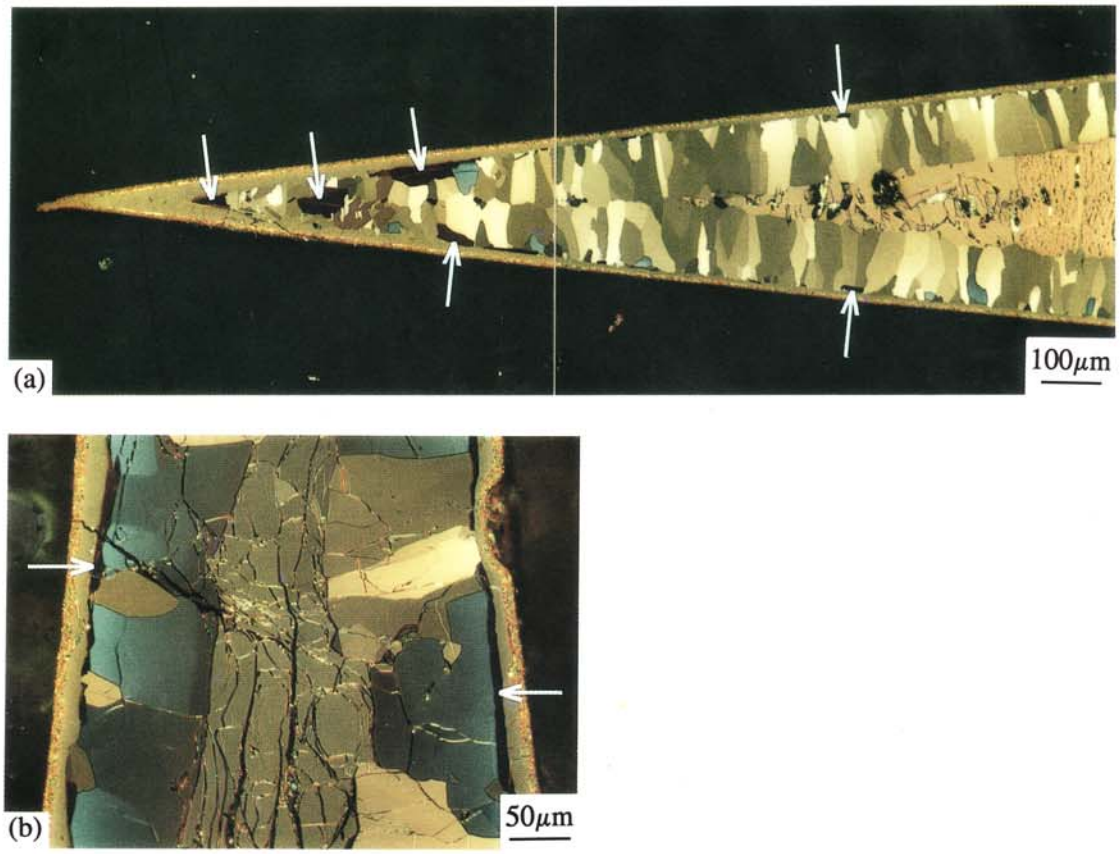

Fig. 3. Wedge-type sample prepared in a two-step annealing process at 1180°C. Polarized light. (a) Microstructure after the first annealing step (450 h) in N_2. The ζ-Hf_4N_{3-x} grains (dark crystallites marked with arrows) form as single, rather than interconnected, grains and most frequently at near-tip positions. (b) Microstructure after the second annealing step (600 h) in Ar atmosphere. ζ-Hf_4N_{3-x} forms diffusion bands (arrows) with interconnected grains.

annealing time of 100 h and a sample 1 mm thick. However, in a 0.1 mm thick sample the phase band thickness increases to 3.9 μm, which would of course be observable in the light-optical microscope. Furthermore, ζ-Hf_4N_{3-x} was not detected by Billy and Teyssedre [4] with XRD in Hf/HfN mixtures heat treated at 1200°C for 100 h, which, too, is a relatively short time in view of the low diffusion rate of nitrogen in hafnium nitrides.

Additional investigations were therefore made in the present study using wedge-shaped Hf samples. In such samples considerable layer thickness enhancement can be obtained as a result of the restricted diffusion geometry (for a detailed description see Ref. [5]). Depending on the annealing conditions, the layer thickness for the ζ-Hf_4N_{3-x} phase is about 20 times that for semi-infinite diffusion geometry (similar results were obtained for the V–C system where the ζ-V_4C_{3-x} phase band was observable by light-optical metallography only for thin wedge thicknesses [10]).

For present purposes a wedge-type Hf sample 15 mm long with a thickness of approx. 1 mm at one end was reacted in 10 bar N_2 at 1160°C for approx. 500 h. After cooling to room temperature the sample was re-heated again to 1160°C for about 500 h. Under these time/temperature conditions a wedge-type hafnium diffusion couple still has an α-Hf(N) core at greater thicknesses which can cause fissures in the sample, probably because of the peculiar thermal expansion behavior of the core. Indeed, upon cooling and re-heating the Hf–N developed fissures where the wedge was thick but remained intact where it was thinner and α-Hf(N) was no longer present. Microstructures representative of the two positions (cracked, whole) are shown in Figs 2(a) and 2(b). It can be seen that below the original surface the ζ-Hf_4N_{3-x} phase did not develop as a band but instead in the form of needles visible as hatched areas and sometimes as individual crystallites [Fig. 2(a)]. In contrast to the hatchings just below the original surface, ζ-Hf_4N_{3-x} also formed under the secondary surface which resulted from the cracking [Fig. 2(b)]. This indicates that the supply of nitrogen influences the phase band structure at lower temperatures. To investigate this a two-step experiment was performed: first wedge-type and thin plane sheet samples were reacted with nitrogen at 1180°C for 450 h and then annealed in Ar at the same temperature for 600 h. For this experiment the heating and cooling cycles

were effected in slow temperature increments and decrements in a heavy Mo crucible so that sample breakage could sometimes be avoided. The microstructure of the wedge after the N_2 annealing step is shown in Fig. 3(a). At near-tip positions the ζ-Hf_4N_{3-x} phase frequently forms as individual grains rather than the expected layer. Upon heating in Ar atmosphere, however, a nearly continuous ζ-Hf_4N_{3-x} layer formed [Fig. 3(b)]. If the second step was performed in nitrogen atmosphere no significant difference to the first cycle could be detected concerning the formation of ζ-Hf_4N_{3-x} phase. Apparently the supply of nitrogen rather than the orientation of the η-Hf_3N_{2-x} grains has an influence on the formation characteristics of this phase. According to layer growth kinetics in diffusion couples it does indeed follow that a decrease of supply of diffusing species at the surface causes the inner phase bands to broaden. Although it seems that these features of ζ-Hf_4N_{3-x} formation below ca. 1250°C need additional experimental investigation, for the present it appears that ζ-Hf_4N_{3-x} definitely is stable at temperatures below 1200°C, contrary to reports in the literature [4, 7].

3.2. *Homogeneity ranges of phases*

EPMA has proved to be an exceptionally well-suited tool for the determination of homogeneity ranges of phases from diffusion couples, but due to restrictions in lateral resolution it is difficult to measure the homogeneity ranges of narrow phase bands. An additional difficulty is the fact that the microprobe operates on a wt% basis so that the light-element analysis—itself difficult to perform quantitatively—is inherently subject to substantial errors.

Such a situation prevails in the Hf–N system—where the maximum nitrogen content is about 7 wt% (for δ-HfN_{1-x})—and especially for ζ-Hf_4N_{3-x}, which has a very narrow homogeneity region. Wedge-shaped samples, however, with the advantage of width enhancement could assure a sufficient number of data collection points within the phase band to yield reliable information on the homogeneity regions. Such a measurement is shown in Fig. 4 together with the corresponding microstructure. The statistically necessary number of data points could be obtained in each phase band. The homogeneity region of ζ-Hf_4N_{3-x} was determined to be 38.9–39.6 at% N whereby the absolute accuracy (the position in the phase diagram) is about ± 1 at% N at best, which can, however, be calibrated by preparation and analysis of single-phase samples [5]. The homogeneity ranges of the hafnium nitride phases are given in Table 1. Within the accuracy of the results the phase boundaries of the subnitride phases are constant with temperature. The difference between the homogeneity range of η-Hf_3N_{2-x} and ζ-Hf_4N_{3-x} is interesting, first because both phases are structurally closely related to each other and second because the isostructural titanium nitride phases do not show this behaviour [11].

Chemical analysis of the reference foil gave proof that δ-HfN_{1-x} can indeed attain a hyperstoichiometric composition by nitridation in molecular nitrogen. It was found that, depending on the pressure/temperature relationship, up to 52 at% N ([N]/([Hf] + [Zr]) = 1.08) can be attained. The resulting color was a function of the nitrogen content. High nitrogen pressures resulted in higher nitrogen contents characterized by a dark yellow color which became noticeably paler at the lowest nitrogen content/pressure with the most notable change occurring around the stoichiometric composition. Thus, in a HfN diffusion layer the yellow color becomes darker from the inside towards the outside. In cross sections it was observed that high nitrogen pressures produced a HfN layer composed of two sublayers (see Figs 1 and 2) with a metallographically visible interface. The boundary between those sublayers coincided closely with the sharp color change from dark yellow to pale yellow. It was therefore first assumed that the clearly observable interface was due to the growth of hyperstoichiometric HfN_{1+x} on (sub)stoichiometric HfN_{1-x}. This would imply either a difference in structure between the two compounds or the presence of a substantial outward Hf diffusion against the inward nitrogen diffusion. A structural difference between the two types of HfN could not be found either by XRD or by neutron diffraction [12]. The formation of the outer part by Hf outdiffusion would cause a thinner layer at the edges (corners in the microstructure) than at plane-sheet positions (edges in the microstructure). Since just the opposite was observed it is clear that the outermost dark layer is also formed by nitrogen indiffusion.

Glow-discharge optical emission spectroscopy (GD-OES) depth profiles showed that at this interface carbon, probably from impurities in the gas phase, was accumulated. The carbon content in the outer dark yellow was very low, as a result of the high nitrogen activity that caused carbon to be expelled from the outermost region. Careful metallographic inspection showed that the dark yellow layer extended deeper into the sample than the HfN_{1+x}/HfN_{1-x} interface. At near-tip positions of wedge samples as well as at the corners of the samples of any geometry which were heated under high N_2 pressures, the interface vanished. The transient character of an apparent HfN_{1+x}/HfN_{1-x} interphase boundary could thus be explained by a local carbon pile up in front of the hyperstoichiometric layer. This pile up is caused by a displacement of carbon from the outer region [Fig. 5(a)]. If the sample is fully nitrided, which can be performed with thin plane-sheet samples as well as for the wedge tips, then the nitrogen activity reaches constant values and the carbon-enriched zone homogenizes. At lower nitrogen pressures the nitrogen activity is lower, no carbon-free hyperstoi-

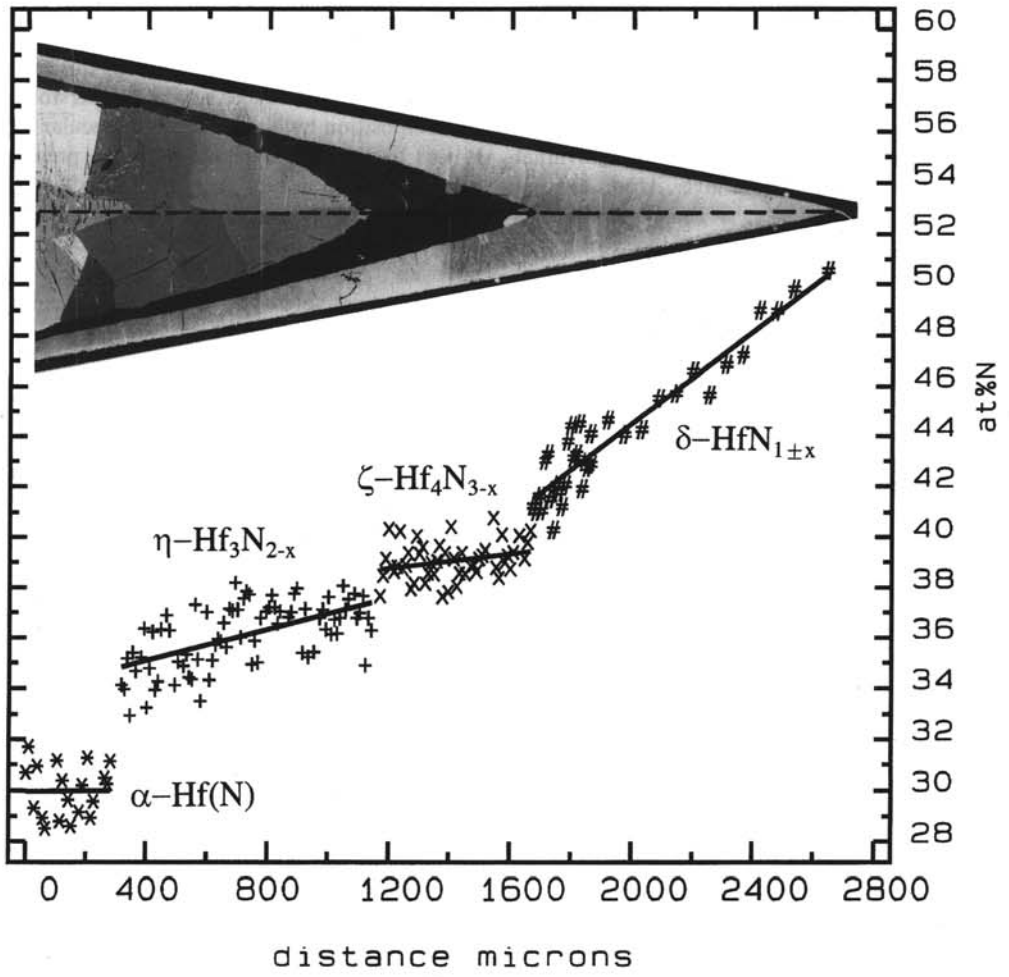

Fig. 4. EPMA scan across the center of a wedge-shaped diffusion couple (indicated in the microstructure on the top). Due to the thickness enhancement of the ζ-Hf_4N_{3-x} phase a large number of data points could be measured for this phase band, giving a statistically reliable homogeneity range of 0.7 at% N (note that, for example, the interval 38–39 at% N corresponds to a difference of only 0.18 wt% N).

chiometric layer is formed, and the carbon content is highest at the surface [Fig. 5(b)]. GD-OES investigations, optical reflectivities and lattice parameter depth profiles in the δ-HfN_{1-x} phase will be presented elsewhere.

Table 1. Homogeneity ranges for hafnium nitride phases. The figures are based on EPMA investigation of several diffusion couples for α-Hf(N), η-Hf_3N_{2-x}, ζ-Hf_4N_{3-x} and the N-poor boundary of δ-HfN_{1-x}. The homogeneity ranges were observed to be constant within the temperature range 1300–1800°C

Phase	Homogeneity range at% N	[N]/[Hf]
α-HfN	0.0–29.7	0–0.42
η-Hf_3N_{2-x}	34.9–37.2	0.54–0.59
ζ-Hf_4N_{3-x}	38.9–39.6	0.64–0.66
δ-HfN_{1-x}	41.5–52.0[a]	0.71–1.08

[a]The composition of δ-HfN_{1-x} at the N-rich boundary depends on the nitrogen pressure vs temperature relationship and was determined by chemical analysis of nitrided 25 μm HfN foil.

All experimental efforts to establish completely carbon-free conditions were unsuccessful. At this stage in the investigation of this phenomenon it seems that the two sublayers respond differently to polishing (the hyperstoichiometric layer often appears to be porous). Because the mechanical properties (similar to the color) also change sharply, but—because of identical crystallographic structure—not discontinuously at the transition point from stoichiometric HfN_{1-x} to hyperstoichiometric HfN_{1+x} a discontinuous behavior is simulated. The appearance of an interface boundary has its origin in carbon contamination and is not causally connected with the double-layer structure.

The phase diagram of the Hf–N system was modified based on the present findings (homogeneity ranges of phases) and is given in Fig. 6.

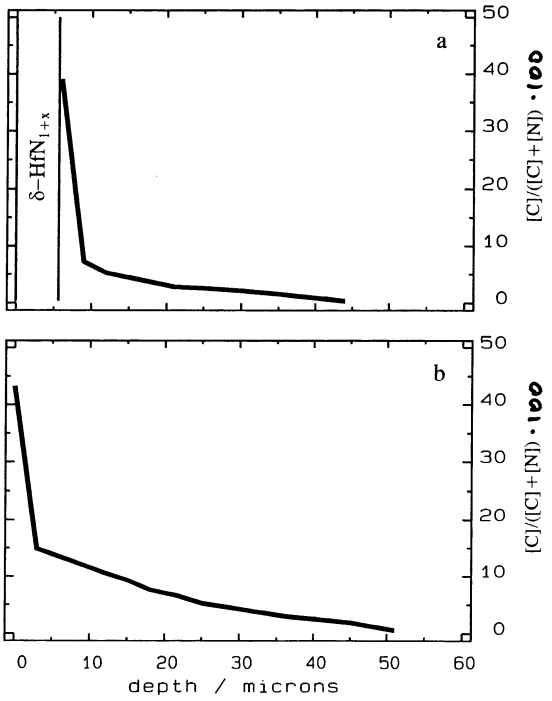

Fig. 5. Carbon depth profiles within the diffusion band of δ-HfN_{1-x} obtained from lattice parameter measurements and the approximation of ([C] + [N])/[Hf] = 1. The lattice parameter of $Hf(C_xN_{1-x})$ is a linear function of the [C]/([C] + [N]) ratio [13]. The approximation introduces a small error because the nitrogen content decreases with increasing distance from the surface, but it has a much weaker influence on the lattice parameter ($HfN_{0.80}$:0.4525 nm, $HfN_{1.00}$:0.4520 nm) than the carbon content (HfC:0.4634 nm). To increase the observability of the carbon influence the samples were intentionally contaminated with extra carbon by heating a graphite cylinder in the autoclave prior to the experiments. (a) Depth profile in a sample nitrided for 120 h at 1700 C and 30 bar N_2. In the hyperstoichiometric layer, where the approximation given above is not applicable, because of a steep decrease of the lattice parameter, the carbon content is negligible (according to GD-OES). The carbon content is highest just next to the HfN_{1+x}. (b) Depth profile in a sample nitrided for 120 h at 1700 C and 1.6 bar N_2. No hyperstoichiometric layer forms under these conditions. The carbon contamination is highest at the surface and is identical to the maximum shown in Fig. 5(a).

3.3. *Layer growth and diffusivities*

The phase band widths of the phases η-Hf_3N_{2-x}, ζ-Hf_4N_{3-x} and δ-HfN_{1-x} were measured as a function of temperature and time. If, for the latter, an interface boundary could be observed within the phase band both sublayers were treated as a single layer. No differences in layer thickness could be found whether the experiment was carried out at low pressures (no interface) or at high pressures (interface present at positions away from the corners).

It was shown recently [5] that the plane-sheet geometry significantly influences the diffusion layer width. A formalism dependent on differential equations was used in the form of a computer code [14] which allows the calculation of the layer width as a function of time and temperature in multiphase samples of plane-sheet geometry, assuming that nitrogen is the only diffusing species. From a series of samples with semi-infinite diffusion geometry this is only possible if one diffusivity is known (compare Refs [15, 16]). However, if several plane-sheet samples with different thicknesses are prepared under the same conditions or—even better—if a wedge-type sample is prepared, then the diffusivities in all phases can be obtained from the measurement of the layer widths because the parabolic rate constant k in the expression $x = k \times \sqrt{t}$, where x is the layer thickness and t is the time, is then a function of time. Application of different diffusion times or different thicknesses can then yield the diffusivities in all phases. A detailed description will be given elsewhere [14]. The formalism was tested by application to the Zr–O system where reliable oxygen diffusivity data exist [17]. Excellent agreement between the so-obtained data and the literature data was found.

The average concentration-independent chemical diffusion coefficients of nitrogen, D_N, in the hafnium nitride phases are shown in Fig. 7. A clear Arrhenius dependency of the D_N values was observed. The respective expressions for D_N are

in δ-HfN_{1-x}: $D_N = 0.02 \times \exp(2.70\,\mathrm{eV}/k_B T)$

in ζ-Hf_4N_{3-x}: $D_N = 0.14 \times \exp(2.74\,\mathrm{eV}/k_B T)$ and

in η-Hf_3N_{2-x}: $D_N = 0.54 \times \exp(2.73\mathrm{eV}/k_B T)\mathrm{cm}^2/\mathrm{s}$,

where k_B is the Boltzmann constant.

For δ-HfN_{1-x} a concentration dependency of D_N is to be expected because of the large vacancy concentration variation (compare Ref. [5]). Thus, the value obtained can be regarded as the nitrogen

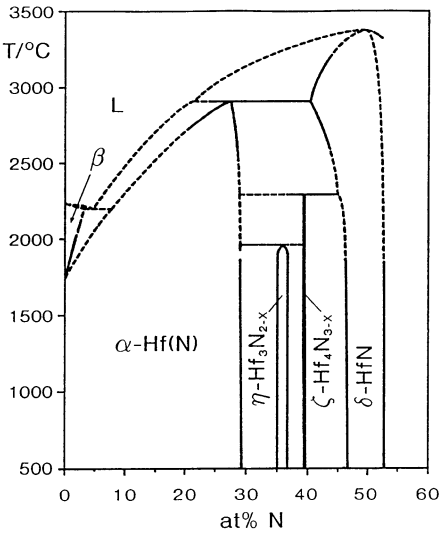

Fig. 6. Phase diagram of the Hf–N system compiled by Okamoto [7] and revised for the range $T < 1800$ C in accordance with the present results.

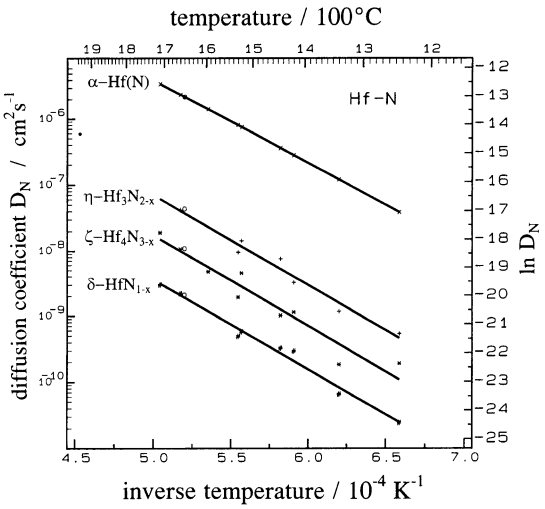

Fig. 7. Concentration-independent nitrogen diffusion coefficients D_N in the various hafnium nitride phases. The data set represented by the circles at $T = 1650°C$ was obtained from a wedge-type sample from which also the D_N in the α phase could be determined (see text). All other data points were obtained from plane sheet samples under the assumption that the activation energy of the α phase is $Q_\alpha = 2.5$ eV. The influence of the activation energy chosen for α on the results for the D_N (and D_0 and Q) of the nitride phases is, however, very weak and alters the results insignificantly upon calculation if taken differently.

diffusivity of an intermediate composition of $HfN_{\sim 0.88}$.

From the results it can be seen that for the three hafnium nitride phases the activation energy of nitrogen diffusion decreases only slightly with decreasing nitrogen content (this decrease is near the limit of accuracy of the determination). This points to an identical diffusion mechanism of migration via vacant octahedral sites. Thus a difference in nitrogen diffusivity is reflected by the frequency factor which covers the jump probability and which is different because of the different occupancies of nitrogen positions in the different phases. This is consistent with the constant activation energies indeed observed for the carbon diffusion in TiC_{1-x} and ZrC_{1-x} [18] as well as for NbC_{1-x} [19].

Acknowledgements—The authors would like to thank Dr R. Kalista, Teledyne Wah Chang, Leichtenstein, for supplying Hf sheet and Mr M. Bohn, IFREMER, France, for assistance with the microprobe measurements. Mrs C. Jelinek helped with the preparation of the manuscript. The work was supported by the Austrian National Science Foundation FWF under project No. 8487 and through the French–Austrian research contract A11.

REFERENCES

1. P. Ettmayer and W. Lengauer, in *Ullmann's Encyclopedia of Industrial Chemistry*, Vol. A16, p. 341–361. Weinheim, Germany (1991).
2. E. Rudy, *Metall. Trans.* **1,** 1249 (1970).
3. E. Rudy and F. Benesovsky, *Monatsh. Chem.* **92,** 415 (1961).
4. M. Billy and B. Teyssedre, *Bull. Soc. Chim. Fr.* **1,** 1537 (1973).
5. W. Lengauer, D. Rafaja, R. Täubler, C. Kral and P. Ettmayer, *Acta metall. mater.* **41,** 3505 (1993).
6. M. E. Straumanis and C. A. Faunce, *Z. Anorg. Allg. Chem.* **353,** 329 (1967).
7. H. Okamoto, *Bull. Alloys Phase Diagr.* **11,** 146 (1990).
8. A. J. Perry, *Powder met. Int.* **19,** 29 (1987).
9. R. Täubler, S. Binder, M. Groschner, W. Lengauer, and P. Ettmayer, *Mikrochim. Acta I* **107,** 337 (1992).
10. H. Wiesenberger, W. Lengauer and P. Ettmayer, *8th Int. Conf. High-Temperature Materials*, April (1994), Coll. Abstr., to be published.
11. W. Lengauer, *Acta metall. mater.* **39,** 2985 (1991).
12. P. Rogl, P. Fischer and W. Lengauer, *Prog. Rep. Annual Progress Report 1993*, Labor für Neutronenstreuung, ETH Zürich and Paul Scherrer Institute, LNS-170, Feb. (1994).
13. W. Lengauer, S. Binder, K. Aigner, P. Ettmayer, A. Guillou, J. Debuigne and G. Groboth, *J. Alloys Comp.* **217,** 137 (1995).
14. D. Rafaja, W. Lengauer and P. Ettmayer, *Acta mater.*, in press.
15. W. Jost, *Diffusion in Solids, Liquids, Gases*. Academic Press, New York (1952).
16. J. Philibert, *Atom Movements, Diffusion and Mass Transport in Solids*. Les Editions de Physique, Les Ulis (1991).
17. R. E. Pawel, *J. Electrochem. Soc.* **126,** 1111 (1979).
18. F. J. J. van Loo, W. Wakelkamp, G. F. Bastin and R. Metselaar, *Solid State Ionics* **32,** 824 (1989).
19. W. Lengauer, *J. Alloys. Comp.* **229,** 80 (1995).